Effects of Lead Exposure on Blood Electrical Impedance Spectroscopy of Mice

Binying Yang
1 Ninghai First Hospital, Zhejiang Province; 2 School of Medicine Ningbo University
Jia Xu
School of Medicine, Ningbo University
Shao Hu
Ninghai First Hospital, Zhejiang Province
Boning You
Ninghai First Hospital, Zhejiang Province
Qing Ma (maqing@nbu.edu.cn)
School of Medicine, Ningbo University

Research Article

Keywords: Lead-exposed, Blood, Electrical impedance spectroscopy, Characteristic frequency

Posted Date: June 15th, 2021

DOI: https://doi.org/10.21203/rs.3.rs-583512/v1

Effects of lead exposure on blood electrical impedance spectroscopy of mice

Binying Yang[1, 2], Jia Xu[2], Shao Hu[1], Boning You[1], Qing Ma[2*]

1 Ninghai First Hospital, Zhejiang Province, Ninghai 315600, China.

2 School of Medicine, Ningbo University, Zhejiang Province, Ningbo 315211, China.

* Correspondence: Qing Ma (maqing@nbu.edu.cn)

Abstract:

Background: Lead is a nonessential heavy metal, which can inhibit heme synthesis and has significant cytotoxic effects. Nevertheless, its effect on the electrical properties of red blood cells (RBCs) remains unclear. Consequently, this study aimed to investigate the electrical properties and the electrophysiological mechanism of lead exposure in mouse blood using Electrical Impedance Spectroscopy (EIS).

Methods: AC impedance method was used to measure the electrical impedance of healthy and lead exposure blood of mice in 0.01-100 MHz frequency range. Data characteristic of the impedance spectrum, Bodes plot, Nyquist plot and Nichols plot, and three elements equivalent circuit model were used to explicitly analyze the differences in amplitude-frequency, phase-frequency, and the frequency characteristic of blood in electrical impedance properties.

Results: Compared with the healthy blood in control mice, the changes in blood exposed to lead was as follows: (I) the hematocrit decreased; (II) the amplitude-frequency and phase-frequency characteristics of electrical impedance decreased; (III) the characteristic frequencies (f_0) were significantly increased; (IV) the electrical impedance of plasma, erythrocyte membrane, and hemoglobin decreased, while the conductivity increased.

Conclusion: Therefore, EIS can be used as an effective method to monitor blood and RBCs abnormalities caused by lead-exposure.

Key Words: Lead-exposed; Blood; Electrical impedance spectroscopy; Characteristic frequency

Background

Lead is a heavy metal material that has been widely applied in pottery, lead welding, dyes, and cosmetics [1]. Exposure to the high concentration of lead may cause damage to the nervous system, digestive system, blood system, kidney, and other organs [2-4]. A new analysis by the Institute for Health Metrics and Evaluation (IHME) has estimated that 815 million children worldwide have a high concentration of lead in their bloodstream [5]. Clinical evidence suggested that severe chronic lead poisoning can lead to toxic encephalopathy and extensor muscle weakness phenotype of nervous system damage, while acute lead poisoning can lead to damage to the blood-brain barrier, disturbance of messenger molecules (cAMP and NO) and protein kinase, loss of connectivity density between brain endothelial cells, and eventually brain edema. Lead toxicity can induce atrophy of renal cortex, fibrosis of renal tubules, inclusion bodies in renal proximal nuclei, and induce diabetes and amino acid urine [6, 7]. Moreover, high blood lead levels can lead to abortion, low birth weight, reduced sperm number, and motility resulting in reproductive toxicity [8].

Hematological studies have shown that 95% of blood lead is bound to erythrocyte membrane and hemoglobin, while the rest (5%) is found in the plasma. Lead can affect heme synthesis by interfering with porphyrin metabolism disorder. This can eventually cause the compensatory proliferation of erythroblasts in bone marrow, increase reticulocyte and alkaline granulocyte and decrease of the numbers of erythrocytes and leukocytes in the blood, which in turn lead to hemolytic anemia [9]. Hematological abnormalities include hematocrit (Hct), zinc protoporphyrin (ZPP), Na^+-K^+-adenosine triphosphatase (Na-K-ATPase), and others [10]. ZPP and free protoporphyrin IX in RBCs are sensitive and reliable indicators of porphyrin metabolism and lead exposure. Slobozhanina *et al.* pointed out that the low concentration of lead acetate can change the physicochemical state of proteins and lipids in erythrocyte and lymphocyte membranes. Lead acetate affects the enzymatic activity and the functionality of membrane receptors and ion channels, thus modulating the intracellular space and cell functions present at the molecular level [11]. Kasperczyk *et al* evaluated 154 occupational lead-exposed workers and 129 healthy workers and found that oxidative stress is essential during lead poisoning pathogenesis. In addition, occupational lead-exposed workers showed whole blood viscosity, erythrocyte aggregation, and deformability, malondialdehyde, lipofuscin, and glutathione contents compared to controls [12]. Moreover, Ahyayauch *et al.* measured the membrane properties of rat erythrocytes and erythrocyte membrane ghosts by either chronic or acute Pb^{2+} treatments and found that 1.8 μM Pb^{2+} could directly increase cell membrane permeability, thereby increasing hemolysis [13]. Sun and colleagues also pointed that 1-100 μmol/L $PbCl_2$ could induce the reversible increase of $[Ca^{2+}]_i$ level in lymphocytes by activating calmodulin (CaM), thus suggesting the lead affects the physiological function of the cell membrane [14]. However, despite these documented molecular insights into the lead on blood or immunocytes, there is still no report on the electrical properties of lead exposure in mouse blood. The electrophysiological mechanism of lead-exposed RBCs remains unclear and needs to be further explored.

Electrical impedance spectroscopy of cells is widely accepted as a label-free, non-invasive, and quantitative analytical method for the assessment of live biological cells' electrical properties and heterogeneity [15]. Kim *et al*. designed a microfluidic-based physiometer capable of measuring the electrical characteristics of the blood, i.e., the cytoplasm resistance ($R_{cytoplsm}$), plasma resistance (R_{plasma}), and RBC membrane capacitance based on EIS. Combined with image processing, the effects of the hematocrit and

RBC deformability on the whole blood viscosity have been previously reported [16]. In their systematical analysis, Babić *et al.* pointed out that all-natural polyphenol flavonoids share a common non-specific mechanism of platelet activation and aggregation inhibition by the impedance spectrum and flow cytometry, which is related to their lipophilicity and membrane stability. It is of great significance to guide the formation and prevention of thrombosis in cardiovascular diseases [17]. With the development of impedance spectroscopy technology, EIS has been widely used in hematology detection, clinical diagnosis, disease mechanism exploration, and drug research and development.

In this study, we investigated the electrical properties and the electrophysiological mechanism of lead exposure in mouse blood using a lead-exposed mouse model and AC impedance measurement technology. Impedance spectrum bodes diagram, Nyquist diagram, Nichols diagram, and three-element equivalent circuit model were comprehensively analyzed to establish the evaluation of blood electrophysiological parameters on lead exposure. A comprehensive impedance spectrum, Bodes plot, Nyquist plot, and Nichols plot, and three elements equivalent circuit model analysis were used to evaluate the blood electrophysiological parameters on lead exposure. This study provides a novel research method for the application of impedance spectroscopy in clinical diagnosis and lead poisoning treatment.

Results

Effect of lead exposure on electrical impedance spectroscopy and Nyquist plots of blood

The blood Hct of the exposure group (37.52 ± 3.67 %) was 9.66 % ($p<0.05$) lower than that of the control group (41.53 ± 3.6 %), which suggested that the number of RBCs decreased due to lead exposure. The change was consistent with lead-exposed blood of different species, such as *Algerian Mice* [18], *Apodemus sylvaticus* [19], *Parus major* [20], adults [21], and children [22].

Figure 1A clearly shows the relationship between the 3D spectrum and 2D projection (**Figure 1B-D**) of electrical impedance spectrum in lead-exposed blood. The real part of the Impedance-Frequency spectrum [$Z'(f)$ curve] is presented in **Figure 1B**. Due to the low frequency of the electric field, RBCs have enough time to respond to the electric field and produce complete polarization at the low excitation frequency (< 0.1MHz). The polarized RBCs membrane has capacitor characteristics; the capacitance reactance [$1/(\omega C_m)$] decreases with increasing frequency. As current is hindered by the high impedance of RBCs membrane, it consequently flows through the extracellular plasma, which is expected due to the low impedance properties. Therefore, the limit of the real part of impedance at low frequency (Z'_{0C} *and* Z'_{0E}) reflects the electrical properties of the blood plasma, and RBCs suspension shows high impedance characteristic of capacitance at low frequencies. With increasing excitation frequency from 0.1 to 10 MHz, the capacitance of the cell membrane and the impedance of RBCs suspension begins to decrease due to incomplete polarized RBCs. Overall, the decreasing trend of the real part of impedance (Z') generally occurred between 0.1-10 MHz, which is typically referred to as β dispersion. There are two sub-relaxations in β dispersion; the 1st and 2nd characteristic frequency (f_1 and f_2), which come from the existence of plasma-cytomembrane and cytomembrane-hemoglobin interfacial polarizations, respectively (**Figure 1**). Accompanied by an external electric field, the accumulation of interface charge and the formation of interface polarization phenomena occur due to the interface hindering the charge transfer [23, 24]. The characteristic frequency f_0 performs as

$\sqrt{f_1 \times f_2}$ [25]. At high electric field frequencies (>10 MHz), there is insufficient time for the cells to become polarized, and consequently, the current flows into the intracellular fluid. The $Z'(f)$ curve continues as Z' decreases to $Z'_{\infty C}$, which performs the capacitive short circuit of the membrane. Thus, the limit of the real part of impedance ($Z'_{\infty C}$) represents the electrical characteristics of intracellular hemoglobin [26]. After lead exposure, the $Z'(f)$ spectrum of exposure group shifted down to the low impedance region, which leads to the decreasing of Z'_{0E} and $Z'_{\infty E}$ for characterization of plasma and hemoglobin impedance. The resistance of blood decreased is consistent with the EIS performance of glucose-6-phosphate dehydrogenase deficiency [27]. **Figure 1C** shows the frequency spectrum $Z''(f)$ of the imaginary part of the blood impedance. Below the 0.1 MHz, the Z'' value for the blood is very small and stable, with a value close to zero. From 0.1 to 10 MHz, a single hump is formed at the interface of the cell membrane, and plasma follows from the polarization loss of the induced charges. There are two parameters to the hump: the peak of the imaginary part of impedance (Z''_{PC}) and 1st characteristic frequency (f_{1C}). The curve showed a concave-like increasing tendency from 10 to 100 MHz, with the trend of an upturned tail rise at the higher band, which also appeared in the EIS of frog-blood (Xu *et al.* 2020). While the hump-shaped curve exhibits a downward shift with the value of Z''_{PE} decreases and f_{1E} increases of exposure group. The electrical impedance spectroscopy Nyquist plots present a semicircle arc at low-frequency and an individual semicircle arc with an upturned tail rise at the higher band stretched from right to left (**Figure 1D**). The center of the semicircle below the abscissas [28], together with a graphical definition of the vertices and the height of the semicircle present f_{1C} and Z''_{PC}, respectively. Compared with the control group, the limit of the real part of impedance at low frequency (Z'_{0E}), peak of the imaginary part of impedance (Z''_{PE}), the radius and area of arc were decreased, thus revealing that lead exposure-induced decreased resistance in the blood of mice.

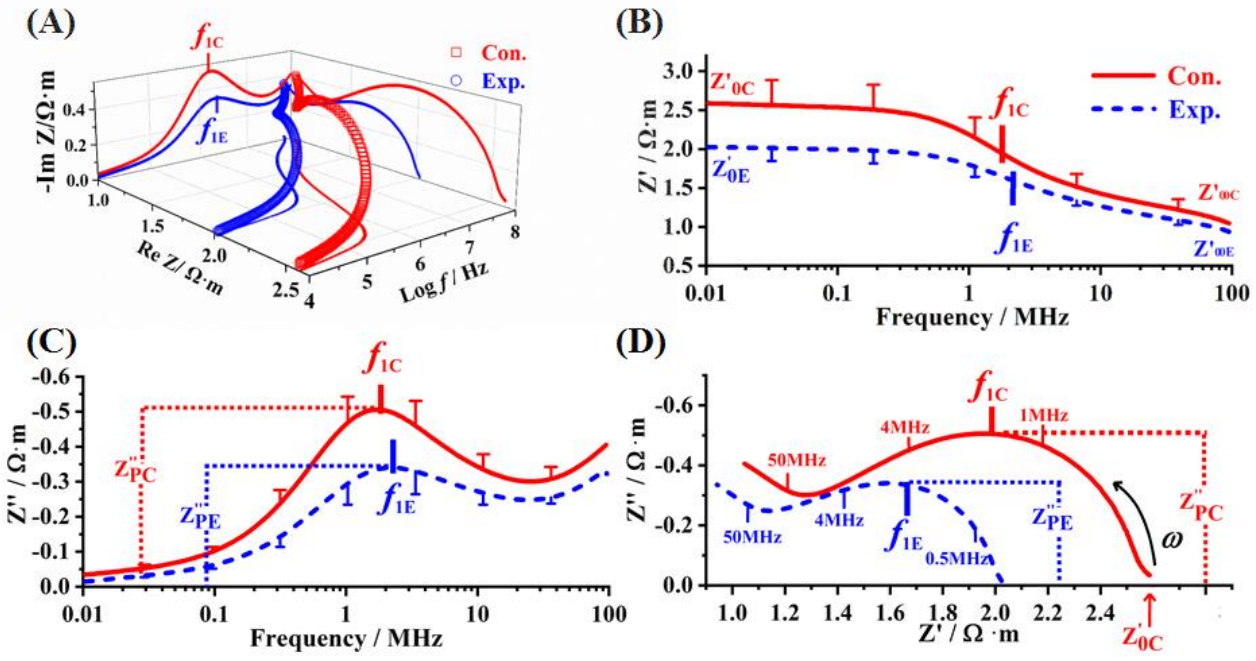

Figure 1. Effects of lead exposure on the real and imaginary parts of electrical impedance spectrum and Nyquist plot of blood in mice. (A) The 3D stereograph of blood impedance spectrum; (B) The $Z'(f)$ curve;

(C) the $\boldsymbol{Z''(f)}$ curve; (D) Nyquist plot. In the 3D curve and axial plane projection of Fig.1 A, hollow squares and solid lines represent the measured spectrum, f–$\boldsymbol{Z'}$ projection (x-y axis, Fig.1 B), f–θ projection (y-z axis, Fig.1 C) and $\mathbf{Z'} - \mathbf{Z''}$ projection (x-z axis, Fig.1 D) of Control group (Con., red) and lead exposed group (Exp., blue). In Figures B-D, the measured spectra of Control and exposure group are represented by solid curves (red) and dotted curves (blue), respectively.

Effect of lead exposure on Bode plots and Nyquist plots of blood

The current flowed through the plasma, erythrocyte membrane, and hemoglobin region as the external electric field increases. The amplitude-phase-frequency 3D stereogram (**Figure 2A**) represents the impedance changes before and after lead exposure to blood. Compared with the control group, the amplitude-frequency curves of Bode plots showed a downshift overall trend (**Figure 2B**). Impedance amplitude at low frequency ($|Z|_{0E}$ = 2.03 ± 0.17 Ω·m) and the Impedance amplitude increment ($\Delta|Z|_E$ = 1.03 ± 0.16 Ω·m) of exposure group had a significant decrease of 21.62 % and 29.93 % compared to control ($|Z|_{0C}$=2.59 ± 0.33 Ω·m, $\Delta|Z|_C$ = 1.47 ± 0.21 Ω·m), respectively. Moreover, the impedance amplitude at high frequency ($|Z|_{\infty,E}$=1.00 ± 0.05 Ω·m) was reduced by 10.71 % but was not statistically significant. The results indicated that blood exposure to lead-induced variable degrees reduction of the electrical impedance in plasma, erythrocyte membrane, and hemoglobin. Moreover, the electrical impedance of extracellular plasma and cell membrane was sensitive to lead exposure. Likewise, the phase-frequency curves of Bode plots showed a significant downward shift compared with the control group (**Figure 2C**). The peak of phase angle (deg) of exposure group (θ_{PE} = -13.23 ± 1.96 deg) was reduced by 17.00 %, and the 2nd characteristic frequency (f_{2E}= 4.96 ± 2.47 MHz) increased by 76.51 % compared with the control group (θ_{PC}= -15.94 ± 0.85 deg, f_{2C}=2.81 ± 0.23 MHz) significantly. The Nichols plots present a semicircle with an upturned tail rise curve from the low- to the high-frequency band, which translated to the left with the increasing of the applied AC electrical field (**Figure 2D**). This is accompanied by the reduction of Logarithm of low-frequency impedance amplitude ($\log|Z|_{0E}$), Peak of phase angle (θ_{PE}/rad), the radius and area of arc, and the increasing of 2nd characteristic frequency (f_2) under the lead exposure blood. Based on the above data, the EIS parameters of blood (Z''_P, θ_P and f_0) are reliable and valid factors for assessing the electrical properties of erythrocyte membrane, which could be used to identify and characterize the charge/discharge processes.

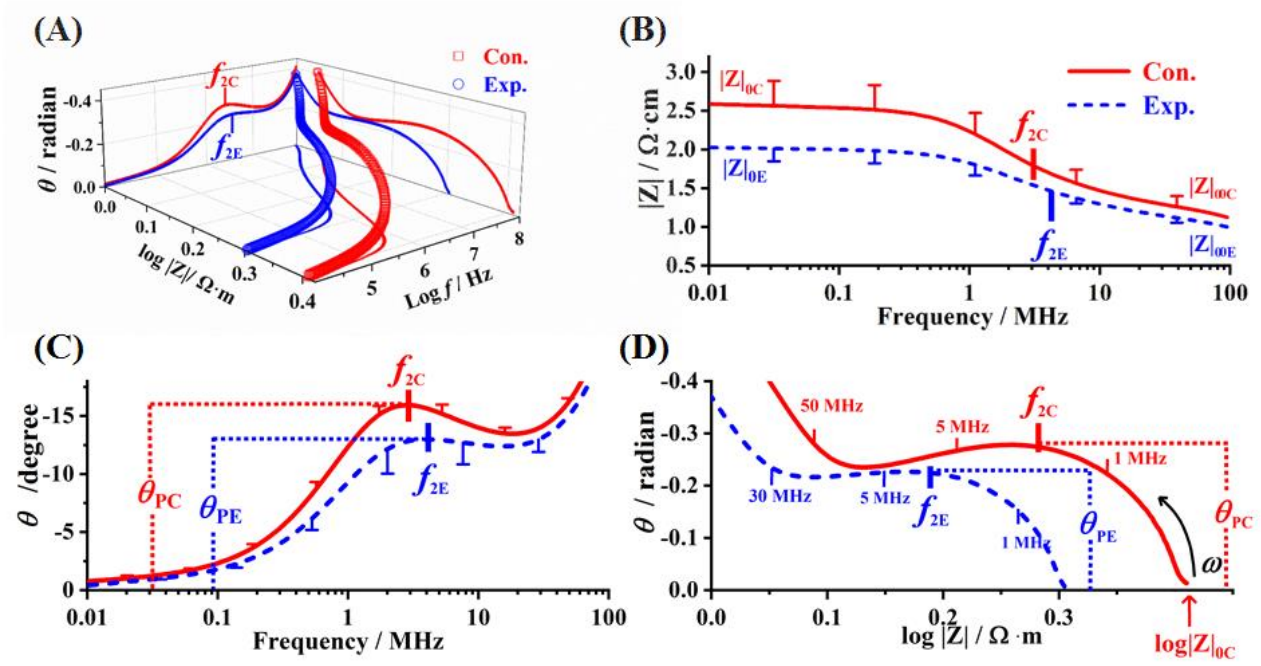

Figure 2. Effect of lead exposure on the Bode and Nichols plots of mice blood. (A) Amplitude-phase-frequency 3D stereogram, (B) Amplitude-frequency curves; (C) Phase-frequency curves; (D) Nichols plots. Labels same as in Figure 1.

Effect of lead exposure on impedance parameters of blood

According to the results from dielectric parameters analysis (**Figure 3** and **Table 1**), there were three changes of lead exposure on blood: (I) the exposure group possessed a reduction of the real part and magnitude of the impedance parameters (Z'_0, Z'_∞, ΔZ, $|Z|_0$, $|Z|_\infty$, $\Delta|Z|$, $\log|Z|_0$) by 22.01%, 10.48%, 29.87%, 21.62%, 10.71%, 29.93% and 33.33%, respectively. (II) Results expressed a significant decrease of the imaginary part and phase angle parameters (Z''_p, θ_p/deg and θ_p/rad) by 26.83%, 17.00%, and 17.86%, respectively. (III) Results showed a significant increase in frequency parameters (f_1, f_2 and f_0) by 27.84%, 76.51% and 48.65%, respectively. These changes of electrical properties are the intuitive feature of the cell membrane and intracellular biochemical reactions by lead exposure. Under the long term lead exposure, the Na^+-K^+ ATPase activity of erythrocyte membrane was inhibited, which induced an imbalance of Na^+-K^+ ion homeostasis in RBCs [29]; the formations of insoluble lead phosphate were synthesized from lead chelating phosphate of the erythrocyte membrane, which may lead to cell hemolysis by increasing the RBC membrane fragility and permeability [30-32]. Consistent with G-6-PD deficiency of RBCs, the changes of biochemical and electrophysiological characteristics were the main factors that induced the significant decrease in RBCs numbers and mass, declined hematocrit (Hct), increased conductivity, and reduced cell impedance [33]. Similarly, we speculate that the changes of phase characteristics and frequency parameters of RBCs induced by lead exposure were due to the weakening of the barrier effect of the high permeability cell membrane. Lead is more likely to interact with δ-aminolevulinic acid dehydratase (ALA-D), xanthinogen oxidase (XOD and iron chelatase (FC) by inhibiting the synthesis of heme and cytochrome [34-36], thus leading to the decrease of hemoglobin, the phosphatidylserine exposure of membrane surface, the shrinkage

of erythrocyte [37] and decrease of volume, as well as the appearance of anemia-like morphological changes [35, 36], eventually causing a significant increase of the characteristic frequency (f_1, f_2, and f_0) of RBCs [38].

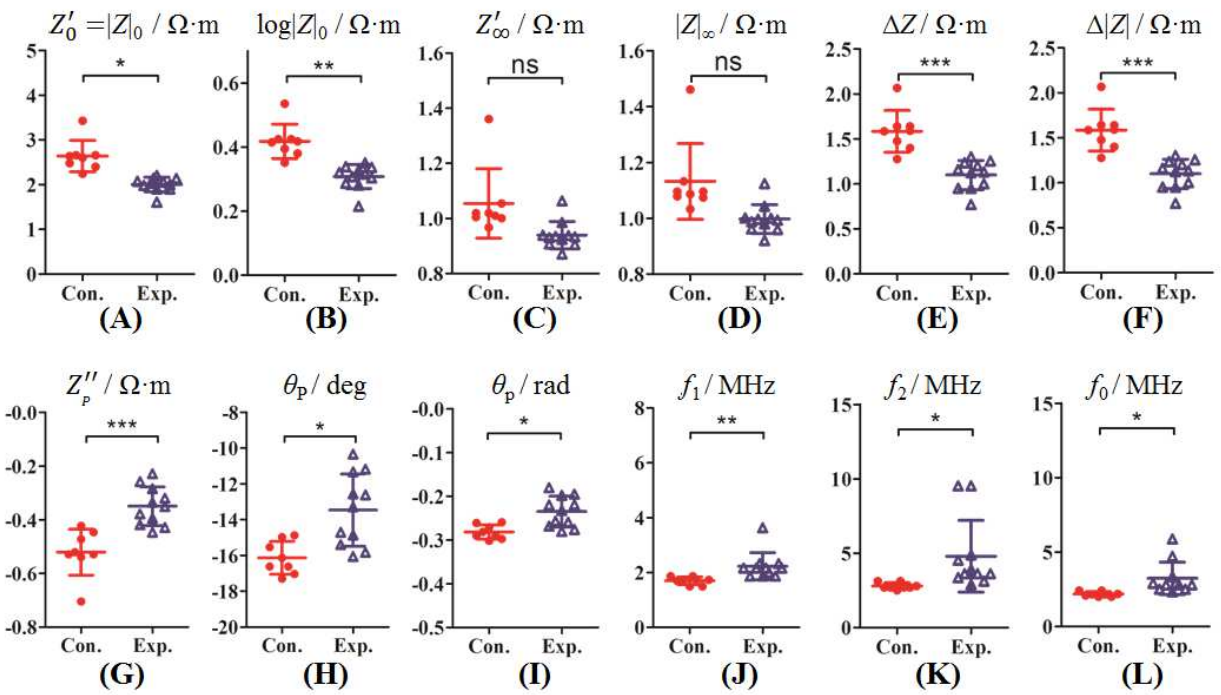

Figure 3. Effect of lead exposed on electrical impedance spectral parameters of blood. (A) Impedance amplitude at low frequency ($|Z|_0$); (B) logarithm of low frequency impedance amplitude (log$|Z|_0$); (C) The limit of the real part of impedance at high frequency (Z_∞'); (D) Impedance amplitude at high frequency ($|Z|_\infty$); (E) Real part increment of electrical impedance ($\Delta Z = Z_0' - Z_\infty'$); (F) Impedance amplitude increment ($\Delta|Z|$= $|Z|_0$- $|Z|_\infty$); (G) Peak of imaginary part of impedance (Z_p''); (H, I) Peak of phase angle (θ_p/deg and θ_p/rad); (J) the 1st characteristic frequency (f_1); (K) the 2nd characteristic frequency (f_2); (L) Characteristic frequency ($f_0 = \sqrt{f_1 \times f_2}$). Solid circles represent Control group (Con.) and hollow triangles represent lead exposed group (Exp.). *Significance at $p < 0.05$, **Significance at $p < 0.01$ and ***Significance at $p < 0.001$, ns indicates no significant difference.

Table 1. The effect of lead exposure on the properties of electrical impedance spectra of mice blood

Parameters	Symbol/ unit	Control (n=10)	Experimental (n=10)	Rate of change (%)
Low frequency limit of real part of impedance	Z_0' / Ω·m	2.59 ± 0.33	2.02 ± 0.17***	-22.01
High frequency limit of real part of impedance	Z_∞' / Ω·m	1.05 ± 0.12	0.94 ± 0.05*	-10.48
Real part increment of electrical impedance	ΔZ / Ω·m	1.54 ± 0.21	1.08 ± 0.16***	-29.87
Impedance amplitude at low frequency	$\|Z\|_0$ / Ω·m	2.59 ± 0.33	2.03 ± 0.17***	-21.62
Impedance amplitude at high frequency	$\|Z\|_\infty$ / Ω·m	1.12 ± 0.12	1.00 ± 0.05*	-10.71
Impedance amplitude increment	$\Delta\|Z\|$ / Ω·m	1.47 ± 0.21	1.03 ± 0.16***	-29.93
Logarithm of low frequency impedance amplitude	log$\|Z\|_0$ / Ω·m	-0.51 ± 0.08	-0.34 ± 0.07***	-33.33

Peak of imaginary part of impedance	Z''_P / Ω·m	0.41 ± 0.05	0.3 ± 0.04***	-26.83
Peak of phase angle (deg)	θ_P / deg	-15.94 ± 0.85	-13.23 ± 1.96*	-17.00
Peak of phase angle (rad)	θ_p / rad	-0.28 ± 0.01	-0.23 ± 0.03*	-17.86
The 1st characteristic frequency	f_1 / MHz	1.76 ± 0.12	2.25 ± 0.52*	27.84
The 2nd characteristic frequency	f_2 / MHz	2.81 ± 0.23	4.96 ± 2.47*	76.51
Characteristic frequency	f_0 / MHz	2.22 ± 0.15	3.30 ± 1.12*	48.65

* $p < 0.05$,** $p < 0.01$, *** $p < 0.001$, compared with the control group.

Effect of lead exposure on the parameters of a three-element equivalent electrical circuit in blood

The cell structural parameters (**Table 2**) were established based on the three-element equivalent electrical circuit model (**Figure 4**), which was obtained through the curves fitting of blood electrical impedance spectrum observation data by Zview2 software. Compared with the control group, the plasma resistance (R_p) and cell membrane capacitance (C_m) significantly decreased by 21.49% and 18.18% under the lead exposure of blood, while the intracellular resistance (R_i) also decreased by 1.10%, but without significant effect.

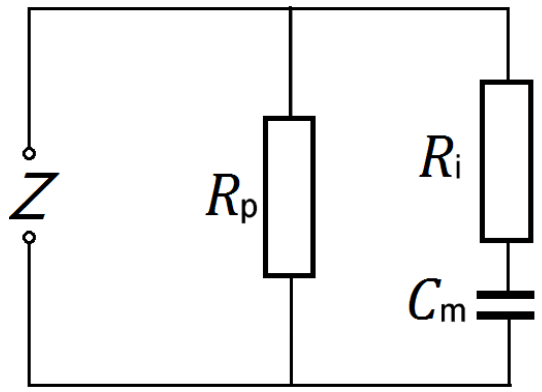

Figure 4. Three-element model of blood, R_p represents plasma resistance, R_i cell interior resistance and C_m cell membrane capacitance.

Table 2. The values of electric components of the established three-element equivalent circuit model

Parameters	Symbol/ unit	Control group	Exposure group	rate of change (%)
Hematocrit	Hct / %	41.53 ± 3.60	37.72 ± 3.5*	-9.18
Plasma resistance	R_p / Ω·m	2.54 ± 0.32	1.99 ± 0.16*	-21.49
Intracellular resistance	R_i / Ω·m	2.53 ± 0.25	2.5 ± 0.33	-1.10
Cell membrane capacitance	C_m / nF·m^{-1}	12.57 ± 1.34	10.29 ± 1.6*	-18.18

* $P<0.05$, compared with the control group.

Conclusion

In summary, this study used the electrical impedance spectrum, Bode plots, Nyquist plots, and Nichols plots data analysis to confirm that lead exposure can reduce the Hct, decrease the impedance and phase angle characteristics, and increase the first and second characteristic frequency of blood in mice. These results provided data support and new diagnosis and treatment methods for the hematotoxicity and the potential electrophysiological mechanism of lead exposure.

Materials

Subjects and blood collection

A total of 20 ICR mice, weighing 27.5 ± 5.1 g on average, were provided by the experimental animal center of Ningbo University. All the animals were housed in an environment with a temperature of 22 ± 1 ℃, relative humidity of 50 ± 1%, and a light/dark cycle of 12/12 hr. All animal studies (including the mice euthanasia procedure) were done in compliance with the regulations and guidelines of Ningbo University institutional animal care and conducted according to the AAALAC and the IACUC guidelines.

The exposure group (n =10) was gavaged with 0.5 ml PbA (250 mg/kg bw) per 24h for 4 weeks; at the same time, the control group (n = 10) was treated with normal saline through identical administration. Blood samples were collected by orbital sinus puncture into heparinized microhematocrit tubes from all mice; blood impedance and hematocrit values were directly determined after pretreatment or centrifugation. Lead acetate (PbA) of AR grade and all other reagents were purchased from Merck (Life Sciences Co., Ltd) unless otherwise stated.

Hematocrit and impedance measurement

Haematocrit (Hct) was measured with micro-haematocrit capillary tubes (1.5 mm outer diameter, 75 mm length; surgical instruments factory of Shanghai Medical Instruments Co., Ltd) in a bench-top haematocrit centrifuge (Haematokrit 210, Germany) for 5 min at 11000 rpm. The hematocrit was calculated using the following equation [39]: Hematocrit (%) = red blood cells volume/blood total volume.

The amplitude $|Z|$ and the phase angle θ of blood were measured by Agilent 4294A Impedance Analyzer (USA), equipped with Agilent 42942A terminal adapter and an Agilent 16192A parallel electrode SMD test fixture; analyzers were controlled by a Lenovo computer. Measurements were made at room temperature. Dispersion characteristic was measured in the frequency range 0.01 to 100 MHz with 124 frequency points. Each run was taken three times under the 0.2V alternating current (AC) voltage, and the data points were the average of these runs. The sample cell was made of clear Plexiglas tube and consisted of a chamber with two parallel platinum plates embedded on both sides, which was customized according to size as follows [40]: 7.7 mm electrode diameter, 8.24 mm distance between electrode pairs, 46.57 mm^2 well area, and 0.38 ml sample volume. The complex impedance was expressed as $Z = |Z| \times e^{-j\theta} = Z' + jZ''$. The real ($Z'$) and imaginary ($Z''$) impedance was calculated as $Z' = |Z| \times \cos\theta$ and $Z'' = |Z| \times \sin\theta$, respectively.

The three-element circuit model for blood impedance analysis

Blood impedance analysis for RBCs was selected according to cellular structures using previously described methods [41, 42]. The impedance of the β dispersion was simulated by a three-element circuit, as shown in **Figure 4**. The values of the three elements of the model, R_p, R_i, and C_m represent plasma resistance, cell interior resistance, and cell membrane capacitance, respectively. These parameters were obtained by curve fitting of blood impedance spectrum data with Zview2 Software. The impedance of the circuit was calculated as follows:

$$Z = \frac{1}{\frac{1}{R_p}+\frac{1}{R_i+\frac{1}{j\omega C_m}}} = Z' + jZ'' \quad (1)$$

Where

$$Z' = \frac{R_p[1+\omega^2 C_m^2(R_i+R_p)R_i]}{1+\omega^2 C_m^2(R_i+R_p)^2} \quad (2), \qquad Z'' = \frac{-\omega C_m R_p^2}{1+\omega^2 C_m^2(R_i+R_p)^2} \quad (3)$$

Statistical analysis

All values were expressed as the means ± standard deviation (SD). The significance of the differences between each value presented by the Control and Lead exposure group was evaluated by the Student *t*-test using SPSS 12.0 software. A p-value < 0.05 was considered to be statistically significant.

Acknowledgments

The authors are grateful to the financial support from the National Natural Science Foundation of China (52007087), the Natural Science Foundation of Zhejiang Province, China (LY20C110001), the Natural Science Foundation of Ningbo City, China (202003N4116), the Fund from the Educational Commission of Zhejiang Province, China (Y202044047), the Fundamental Research Funds for the Provincial Universities of Zhejiang Province, China, and Peiying plan of Ninghai First Hospital, Zhejiang Provinece, China.

Author's contributions

BYY wrote and contributed to the analysis and interpretation of data. BYY and JX wrote the manuscript, collected and analyzed data, performed the experiment, and contributed to the analysis and interpretation of data. BYY, JX and QM wrote the manuscript and discussed the results. BYY, SH, BNY wrote the manuscript, and contributed to its analysis and to the interpretation of data. BYY, QM wrote the manuscript, discussed the results, as well as contributed to its conception, design, analysis, and the interpretation of data. All authors read and approved the final manuscript.

Availability of data and materials

Not applicable.

Declarations

Ethics approval and consent to participate

This study was performed after approval by the Institutional Review Board of school of Medicine, Ningbo University (No. NBU20210015).

Consent for publication

All subjects signed an approved informed consent after the study procedures had been explained and consented to its publication.

Competing interests

The authors declare that they have no competing interests. Authors to whom correspondence should be addressed. Emails: maqing@nbu.edu.cn.

Author details

1 Ninghai First Hospital, Zhejiang Province, Ninghai 315600, China.
2 School of Medicine, Ningbo University, Zhejiang Province, Ningbo 315211, China.

Reference

1. Gidlow D A. Lead toxicity. *Occup Med (Lond)*, 2004; 54(2):76-81.

2. Briffa J, Sinagra E, Blundell R. Heavy metal pollution in the environment and their toxicological effects on humans. *Heliyon*. 2020; 6(9):e04691.

3. Alves Oliveira AC, Dionizio A, Teixeira FB, Bittencourt LO, Nonato Miranda GH, Oliveira Lopes G, et al. Hippocampal Impairment Triggered by Long-Term Lead Exposure from Adolescence to Adulthood in Rats: Insights from Molecular to Functional Levels. *Int J Mol Sci*. 2020; 21(18):E6937.

4. Mani MS, Joshi MB, Shetty RR, DSouza VL, Swathi M, Kabekkodu SP, et al. Lead exposure induces metabolic reprogramming in rat models. *Toxicol Lett*. 2020, 335:11-27.

5. Burki T. Report says 815 million children have high blood lead levels. *Lancet*. 2020; 396(10248):370.

6. Ursula C B, Mark A P. A review of chronic lead intoxication: an unrecognized cause of chronic kidney disease. *Am J Med Sci*. 2004; 327(6):341-347.

7. Das P, Pal S. Lead (Pb), a threat to protein metabolic efficacy of liver, kidney and muscle. *Comparative Clinical Pathology.* 2017; 26: 875–883.

8. Bonde JP, Joffe M, Apostoli P, Dale A, Kiss P, Spano M, et al. Sperm count and chromatin structure in men exposed to inorganic lead lowest adverse effect levels. *Occup Environ Med*, 2002; 59(4):234-242.

9. Gargouri M, Akrouti A, Magné C, El Feki A, Soussi A. Protective effects of spirulina against hemato-biochemical alterations, nephrotoxicity, and DNA damage upon lead exposition. *Hum Exp Toxicol*. 2020; 39(6):855-869.

10. Khalil-Manesh F, Tartaglia-Erler J, Gonick HC. Experimental model of lead nephropathy. IV. Correlation between renal functional changes and hematological indices of lead toxicity. *J Trace Elem Electrolytes Health Dis.* 1994; 8(1):13-19.

11. Gabbianelli R., Fedeli D., Caulini G. C. and Falcioni G. Lead-induced changes in human erythrocytes and

lymphocytes. *J. Appl. Toxicol*. 2005; 25: 109–114.

12. Kasperczyk A, Słowińska-Łożyńska L, Dobrakowski M, Zalejska-Fiolka J, Kasperczyk S. The effect of lead-induced oxidative stress on blood viscosity and rheological properties of erythrocytes in lead exposed humans. *Clin Hemorheol Microcirc*. 2014; 56(3):187-95

13. Ahyayauch H, Sansar W, Rendón-Ramírez A, Goñi FM, Bennouna M, Gamrani H. Effects of chronic and acute lead treatments on the biophysical properties of erythrocyte membranes, and a comparison with model membranes. *FEBS Open Bio*, 2013; 3:212-217.

14. Sun L, Zhao Z, Zhou X, Liu S. The effect of lead on intracellular Ca^{2+} in mouse lymphocytes. *Toxicol In Vitro.*, 2008; 22 (8):1815–1819.

15. Xu Y, Xie X, Duan Y, Wang L, Cheng Z, Cheng J. A review of impedance measurements of whole cells. *Biosens Bioelectron*. 2016; 77:824-836.

16. Kim BJ, Lee YS, Zhbanov A, Yang S. A physiometer for simultaneous measurement of whole blood viscosity and its determinants: hematocrit and red blood cell deformability. *Analyst*. 2019; 144(9):3144-3157.

17. Babić I, Bojić M, Maleš Ž, Zadro R, Gojčeta K, Duka I, et al. Influence of flavonoids' lipophilicity on platelet aggregation. *Acta Pharm*. 2019; 69(4):607-619.

18. Marques CC, Nunes AC, Pinheiro T, Lopes PA, Santos MC, Viegas-Crespo AM, et al. An assessment of time-dependent effects of lead exposure in algerian mice (Mus spretus) using different methodological approaches. *Biol Trace Elem Res*. 2006; 109(1):75-90.

19. Tête N, Afonso E, Bouguerra G, Scheifler R. Blood parameters as biomarkers of cadmium and lead exposure and effects in wild wood mice (Apodemus sylvaticus) living along a pollution gradient. *Chemosphere.* 2015; 138:940-946.

20. Markowski M, Kaliński A, Bańbura M, Glądalski M, Wawrzyniak J, Skwarska J, et al. Effects of experimental lead exposure on physiological indices of nestling great tits Parus major: haematocrit and heterophile-to-lymphocyte ratio. *Conserv Physiol.* 2019; 7(1): coz067.

21. Nakhaee S, Amirabadizadeh A, Brent J, Mehrpour O. Impact of chronic lead exposure on liver and kidney function and haematologic parameters. *Basic Clin Pharmacol Toxicol.* 2019; 124(5):621-628.

22. Kuang W, Chen Z, Shi K, Sun H, Li H, Huang L, et al. Adverse health effects of lead exposure on physical growth, erythrocyte parameters and school performances for school-aged children in eastern China. *Environ Int.* 2020; 145:106130.

23. Wagner, K.W. Erklärung der dielektrischen Nachwirkungsvorgänge auf Grund Maxwellscher Vorstellungen (Explanation of the dielectric aftereffects based on Maxwell's ideas). *Archiv für Elektrotechnik.* 1914; 2(9):371-387.

24. Yardley JE, Kell DB, Barrett J, Davey CL. On-Line, Real-Time Measurements of Cellular Biomass using Dielectric Spectroscopy. *Biotechnol Genet Eng Rev.* 2000; 17(1), 3-36.

25. Pauly H, Packer L. The relationship of internal conductance and membrane capacity to mitochondrial volume. *J Biophys Biochem Cytol.* 1960; 7(4):603-612.

26. Coster HGL, Chilcott TC, Coster ACF. Impedance spectroscopy of interfaces, membranes and ultrastructures. *Biotechnol Bioeng*. 1996; 40(2):79-98.

27. Maha AA. Effect of glucose-6-phosphate dehydrogenase deficiency on some biophysical properties of human

erythrocytes. *Hematology.* 2009; 14(1):38-45.

28. Wang L, Chen L, Wang L, Zhao W, Tang Z, Ma Q. Analysis on Impedance Spectral Characteristic and Equivalent Circuit Model of Mouse Blood. *Journal of Ningbo University (NSEE)*. 2009; 22(4): 573-576.

29. Yücebilgiç G, Bilgin R, Tamer L, Tükel S. Effects of lead on Na^{+}-K^{+} ATPase and Ca^{+2} ATPase activities and lipid peroxidation in blood of workers. *Int J Toxicol.* 2003; 22(2):95-97.

30. Yang K, Chi B, Lin C**.** Effect of lead acetate on growth of murine mesenchymal stem cells. *Journal of Norman Bethune University of Medical Sciences.* 2007; 33(1):116-118.

31. Ahyayauch H, Sansar W, Rendón-Ramírez A, Goñi FM, Bennouna M, Gamrani H. Effects of chronic and acute lead treatments on the biophysical properties of erythrocyte membranes, and a comparison with model membranes. *FEBS Open Bio*. 2013; 3: 212–217.

32. Suljević D, Hodžić-Klapuh L, Handžić N, Fočak M. Morpho-functional alterations in lymphocytes and erythrocytes of Japanese quail due to prolonged in vivo exposure to heavy metal complexes. *J Trace Elem Med Biol.* 2020; 59:126472.

33. Slobozhanina EI, Kozlova NM, Lukyanenko LM, Oleksiuk OB, Gabbianelli R, Fedeli D, et al. lead acetate can change the physicochemical state of proteins and lipids in erythrocyte membranes. *J Appl Toxicol.* 2005; 25(2):109-114.

34. Meyer RP, Podvinec M, Meyer .A. Cytochrome P450 CYP1A1 accumulates in the cytosol of kidney and brain and is activated by heme. *Mol Pharmacol.* 2002; 62(5):1061-1067.

35. Warren MJ, Cooper JB, Wood SP, Shoolingin-Jordan PM. Lead poisoning, haem synthesis and 5-aminolaevulinic acid dehydratase. *Trends Biochem Sci.* 1998; 23(6):217-221.

36. Kaneko M, Kazatani T, Shikata H. Occupational Lead Poisoning in a Patient with Acute Abdomen and Normocytic Anemia. *Intern Med*. 2020; 59(12):1565-1570.

37. Lang F, Gulbins E, Lerche H, Huber SM, Kempe DS, Foller M. Eryptosis, a window to systemic disease. *Cell Physiol Biochem*. 2008; 22 (5–6):373-380.

38. Maskow T, Röllich A, Fetzer I, Ackermann JU, Harms H. On-line monitoring of lipid storage in yeasts using impedance spectroscopy. *J Biotechnol.* 2008; 135(1):64-70.

39. Mondal H, Budh D P. Budh. Hematocrit. In: StatPearls [Internet]. Treasure Island (FL): StatPearls Publishing; 2020 Jan. https://www.ncbi.nlm.nih.gov/books/NBK542276/

40. Xu J, Xie W, Chen Y, Wang L, Ma Q. Dielectric properties of nucleated erythrocytes as simulated by the double spherical-shell model. *Chin. Phys. B.*2020; 29(12):128703.

41. Fricke H, Morse S. The electric resistance and capacity of blood for frequencies between 800 and 4.5 million cycles. *J Gen Physiol.* 1925; 9(2):153-167.

42. Ackmann JJ, Seitz MA, Dawson CA, Hause LL. Specific impedance of canine blood. *Ann Biomed Eng*. 1996; 24(1):58-66.

Figures

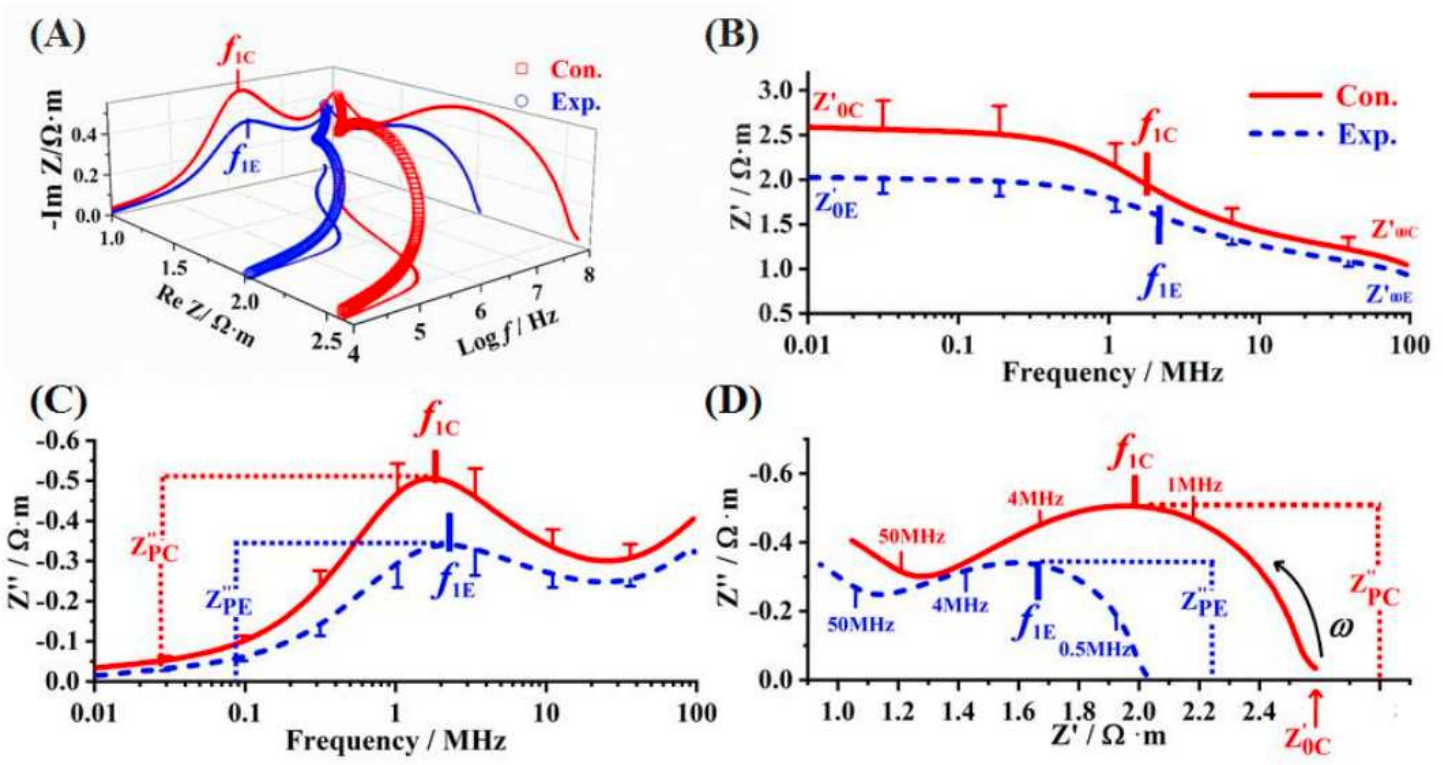

Figure 1

Effects of lead exposure on the real and imaginary parts of electrical impedance spectrum and Nyquist plot of blood in mice. (A) The 3D stereograph of blood impedance spectrum; (B) The Z' (f) curve; (C) the Z" (f) curve; (D) Nyquist plot. In the 3D curve and axial plane projection of Fig.1 A, hollow squares and solid lines represent the measured spectrum, f –Z ' projection (x-y axis, Fig.1 B), f –θ projection (y-z axis, Fig.1 C) and Z' – Z" projection (x-z axis, Fig.1 D) of Control group (Con., red) and lead exposed group (Exp., blue). In Figures B-D, the measured spectra of Control and exposure group are represented by solid curves (red) and dotted curves (blue), respectively.

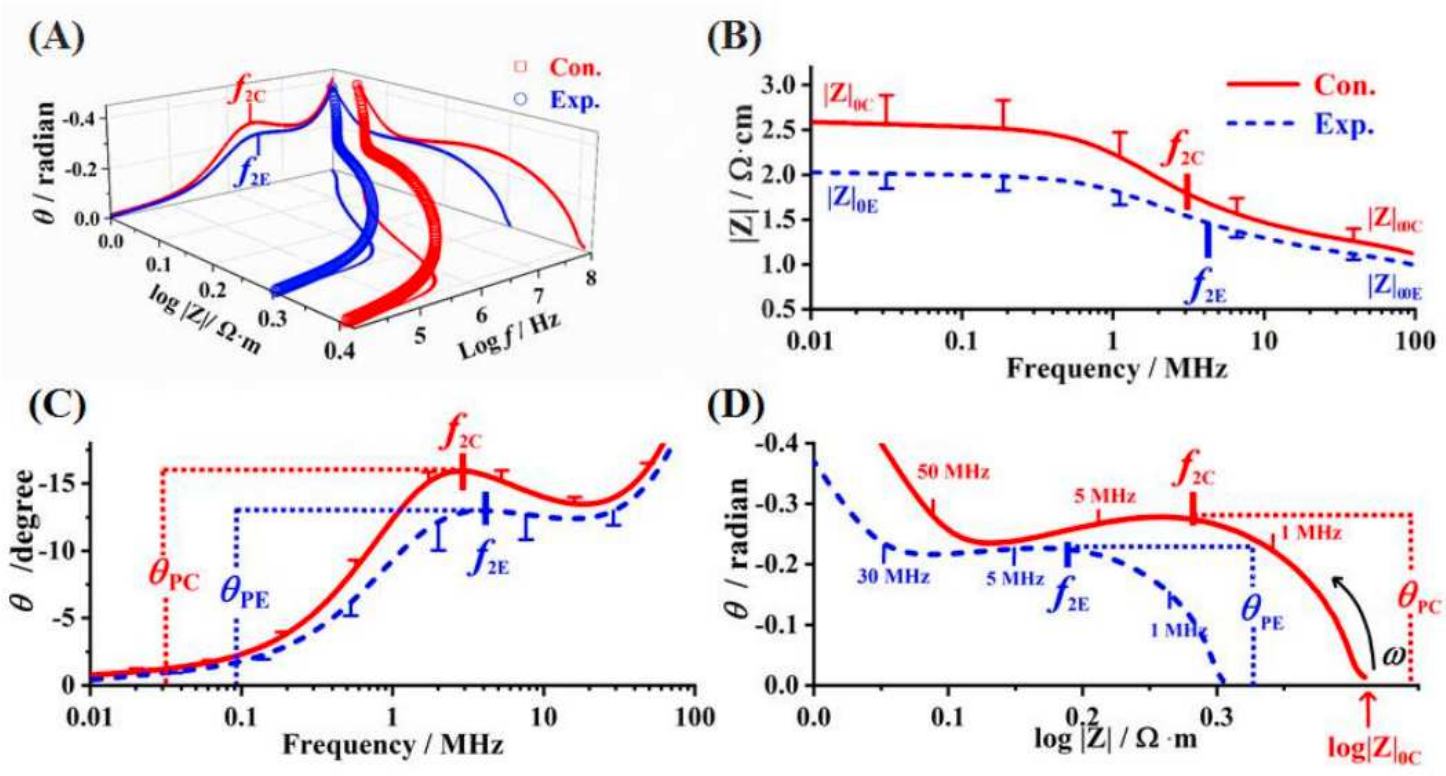

Figure 2

Effect of lead exposure on the Bode and Nichols plots of mice blood. (A) Amplitude-phase-frequency 3D stereogram, (B) Amplitude-frequency curves; (C) Phase-frequency curves; (D) Nichols plots. Labels same as in Figure 1

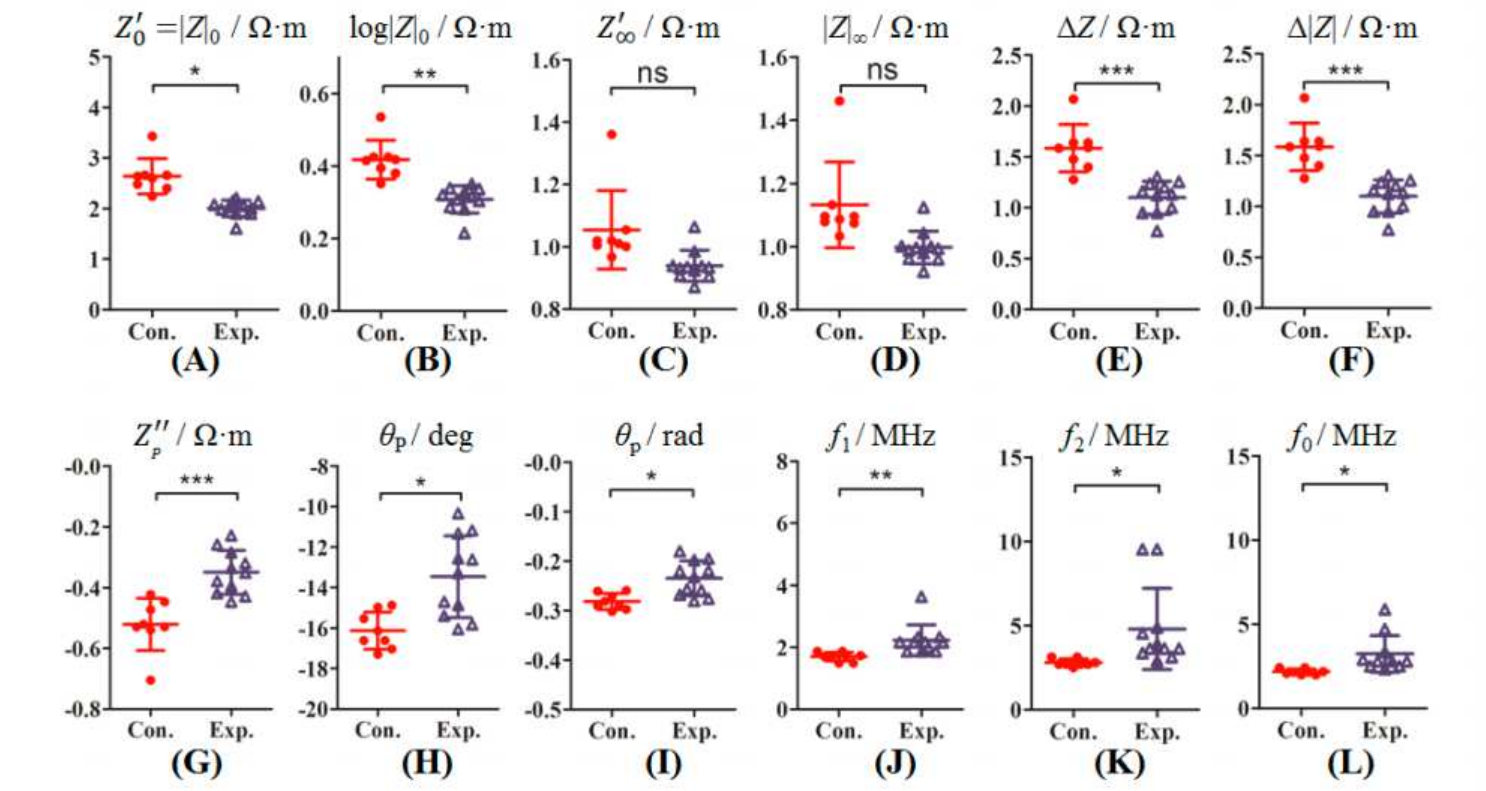

Figure 3

Please see the Manuscript PDF file for the complete figure caption.

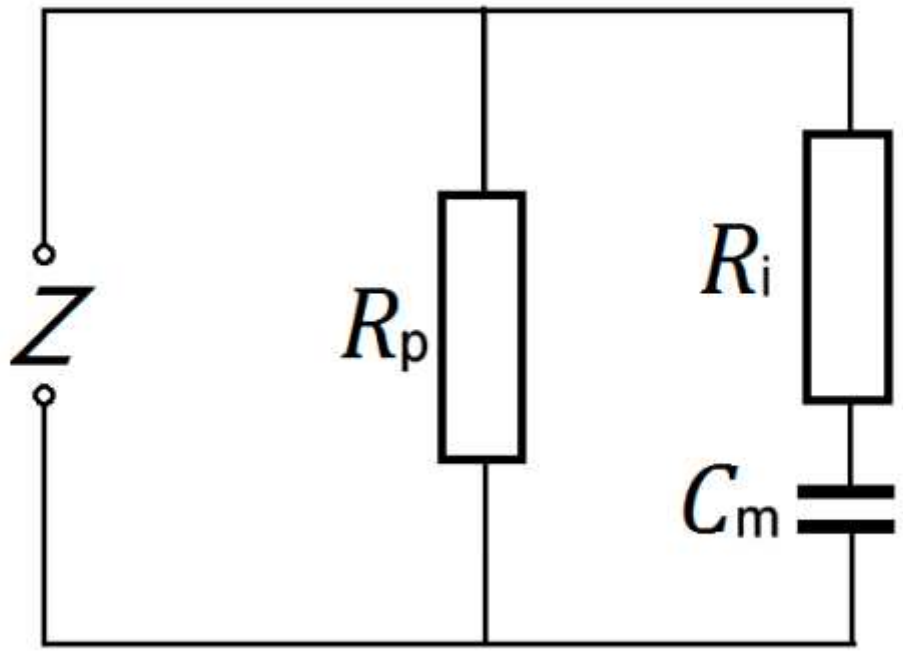

Figure 4

Three-element model of blood, Rp represents plasma resistance, Ri cell interior resistance and Cm cell membrane capacitance.